

Classical limit of the Casimir interaction for thin films with applications to graphene

G. L. Klimchitskaya^{1,2} and V. M. Mostepanenko^{1,2}

¹*Central Astronomical Observatory at Pulkovo of the*

Russian Academy of Sciences, St.Petersburg, 196140, Russia

²*Institute of Physics, Nanotechnology and Telecommunications,*

St.Petersburg State Polytechnical University, St.Petersburg, 195251, Russia

Abstract

The Casimir interaction between two thin material films, between a film and a thick plate and between two films deposited on substrates is considered at large separations (high temperatures) which correspond to the classical limit. It is shown that the free energy of the classical Casimir interaction between two insulating films with no free charge carriers and between an insulating film and a material plate depends on film thicknesses and decreases with separation more rapidly than the classical limit for two thick plates. The free energy of thin films characterized by the metallic-type dielectric permittivity decreases as the second power of separation, i.e., demonstrates the standard classical limit. The obtained results shed light on the possibility to describe dispersion interaction between two graphene sheets and between a graphene sheet and a material plate by modeling graphene as a thin film possessing some dielectric permittivity. It is argued that the most reliable results are obtained by describing the reflection properties on graphene by means of the polarization tensor in (2+1)-dimensional space-time.

PACS numbers: 78.20.-e, 78.67.Wj, 12.20.Ds

I. INTRODUCTION

It is common knowledge that the van der Waals and Casimir forces^{1,2} act between closely spaced material surfaces. These forces are the quantum phenomena caused by the existence of electromagnetic fluctuations. They are also known under the generic name *dispersion forces*. At the shortest separations between the test bodies below a few nanometers, where the relativistic retardation does not play any role, the term *van der Waals forces* is used. At larger separations, where the retardation effects contribute essentially, dispersion forces are usually referred to as the *Casimir forces*. During the last few years the Casimir forces attract much attention as a multidisciplinary subject having prospective applications in condensed matter physics, atomic physics, quantum field theory and in astrophysics and cosmology (see monographs²⁻⁵). Measurements of the Casimir forces between metallic and semiconductor surfaces have also attracted considerable interest (see reviews⁶⁻⁸).

The fundamental theory of the van der Waals and Casimir forces was elaborated by Lifshitz⁹ and is called the *Lifshitz theory*. This theory expresses the free energy and force acting between two thick parallel plates (semispaces) in thermal equilibrium with an environment at temperature T in terms of their frequency-dependent dielectric permittivities. The Lifshitz theory was generalized^{10,11} for an arbitrary number of plane parallel layers of magnetodielectrics characterized by the frequency-dependent dielectric permittivities and magnetic permeabilities. In the last few years the Lifshitz-type theory was developed^{12,13} which describes the van der Waals and Casimir interaction between bodies of arbitrary shape.

Considerable recent attention has been focused on physics of one-atom-thick graphene sheets and other carbon nanostructures which possess unusual electrical, mechanical and optical properties of high promise for many applications.^{14,15} Among different processes and effects which have been investigated, a lot of papers was devoted to calculation of dispersion forces between two carbon nanostructures and between a carbon nanostructure and a body made of some usual material.¹⁶⁻³¹ Many of them used in computations the Lifshitz theory combined with one or other model for the dielectric permittivity of graphene.²⁴⁻²⁹ Otherwise the reflection coefficients of the electromagnetic oscillations on graphene were expressed^{21,23,30,31} in terms of the polarization tensor in $(2+1)$ -dimensional space-time in the framework of the Dirac model (an alternative formalism using Coulomb coupling between

density fluctuations which leads to the same results was also proposed²²). In Ref.³¹ the computational results for the Casimir interaction between two graphene sheets computed using different models of dielectric permittivity on the one hand and the polarization tensor on the other hand have been compared and some disagreements were found. It was concluded that the origin of these disagreements invites further investigation.

Keeping in mind that when using the concept of dielectric permittivity graphene is likened to an ordinary material film of some definite thickness d , in this paper we investigate the thermal Casimir interaction in the presence of thin films. This problem was already discussed in the literature in relation to measurements of the Casimir force. Thus, the van der Waals and Casimir forces acting between Al test bodies covered with Au films were computed at zero temperature.³² In a similar way the role of thin metallic and semiconductor films at zero temperature was investigated in Refs.^{33–35}. At room temperature all these results are applicable for films made of usual materials at separation distances below 1–2 micrometers. They are not applicable to graphene films possessing large thermal effects even at very short separation distances.²² The Casimir force between atomically thin Au films was also calculated using anisotropic dielectric functions obtained with the help of density functional theory.³⁶ This is in line with some dielectric functions used for the description of graphene.^{26,27}

Below we calculate the Casimir interaction in the presence of thin films in the so-called *classical limit*.³⁷ This corresponds to the case of large separations (high temperatures) when only the zero-frequency terms of the Lifshitz formulas provide the total Casimir free energy and force. The obtained results are presented in the closed analytic form and do not depend on a specific choice of the dielectric permittivity, but rather on its behavior at low frequencies. This helps to reveal the physical role of film thickness when applying the concept of the dielectric permittivity to graphene and simplifies comparison with the calculation results obtained using the polarization tensor. Below we consider the thermal Casimir interaction between both isolated films and films deposited on a substrate. The dielectric functions covered by our analysis are both of dielectric and metallic type, i.e., are adapted for theoretical description of both insulators and metals.

The paper is organized as follows. In Sec. II we consider the Casimir interaction between two thin dielectric films and between a dielectric film and a material semispace (either dielectric or metallic). In Sec. III the case of thin metallic films is investigated. Section IV

is devoted to the Casimir interaction between two thick plates (semispaces) coated with thin films. In Sec. V the comparison of our results for thin films with respective results for graphene sheets, obtained using the polarization tensor, are presented. Our conclusions and discussion are contained in Sec. VI.

II. DIELECTRIC FILM INTERACTING WITH ANOTHER DIELECTRIC FILM OR A MATERIAL PLATE

For the needs of this and following sections, we consider the Casimir interaction between two films of thicknesses d_{\pm} with dielectric permittivities $\varepsilon^{(\pm 1)}(\omega)$ separated with a vacuum gap of thickness a with dielectric permittivity $\varepsilon^{(0)}(\omega) = 1$. The films are deposited on two thick plates (semispaces) with respective dielectric permittivities $\varepsilon^{(\pm 2)}(\omega)$ as shown in Fig. 1. The classical limit³⁷ holds at high temperatures or, equivalently, at large separations satisfying the inequalities

$$T \gg T_{\text{eff}} \equiv \frac{\hbar c}{2ak_B}, \quad a \gg a_T \equiv \frac{\hbar c}{2k_B T}, \quad (1)$$

where k_B is the Boltzmann constant. In fact in these inequalities much larger can be replaced with larger (note that at $T = 300$ K $a_T \approx 3.8 \mu\text{m}$ and the classical limit starts from $a \approx 5 \mu\text{m}$).

In the classical limit we can restrict our consideration to the zero-frequency term of the Lifshits formula.² Then the Casimir free energy per unit area of the films is given by^{2,10,11,32}

$$\mathcal{F}(a, T) = \frac{k_B T}{4\pi} \int_0^\infty k_{\perp} dk_{\perp} \sum_{\alpha} \times \ln [1 - R_{\alpha}^{(+)}(0, k_{\perp}) R_{\alpha}^{(-)}(0, k_{\perp}) e^{-2k_{\perp} a}], \quad (2)$$

where $k_{\perp} = |\mathbf{k}_{\perp}|$, \mathbf{k}_{\perp} is the projection of the wave vector on the plane of films, and $\alpha = \text{TM}, \text{TE}$ labels the two independent polarizations of the electromagnetic field, transverse magnetic and transverse electric, respectively. The reflection coefficients on the planes $z = \pm a/2$ are given by

$$R_{\alpha}^{(\pm)}(0, k_{\perp}) = \frac{r_{\alpha}^{(0, \pm 1)}(0, k_{\perp}) + r_{\alpha}^{(\pm 1, \pm 2)}(0, k_{\perp}) e^{-2k^{(\pm 1)}(0, k_{\perp}) d_{\pm}}}{1 + r_{\alpha}^{(0, \pm 1)}(0, k_{\perp}) r_{\alpha}^{(\pm 1, \pm 2)}(0, k_{\perp}) e^{-2k^{(\pm 1)}(0, k_{\perp}) d_{\pm}}}. \quad (3)$$

Here, the reflection coefficients on the various boundary planes are given by

$$\begin{aligned} r_{\text{TM}}^{(n,n')}(i\xi, k_{\perp}) &= \frac{\varepsilon^{(n')}(i\xi)k^{(n)}(i\xi, k_{\perp}) - \varepsilon^{(n)}(i\xi)k^{(n')}(i\xi, k_{\perp})}{\varepsilon^{(n')}(i\xi)k^{(n)}(i\xi, k_{\perp}) + \varepsilon^{(n)}(i\xi)k^{(n')}(i\xi, k_{\perp})}, \\ r_{\text{TE}}^{(n,n')}(i\xi, k_{\perp}) &= \frac{k^{(n)}(i\xi, k_{\perp}) - k^{(n')}(i\xi, k_{\perp})}{k^{(n)}(i\xi, k_{\perp}) + k^{(n')}(i\xi, k_{\perp})}, \end{aligned} \quad (4)$$

where $n, n' = 0, \pm 1, \pm 2$, ξ is the frequency along the imaginary frequency axis and

$$k^{(n)}(i\xi, k_{\perp}) = \left[k_{\perp}^2 + \varepsilon^{(n)}(i\xi) \frac{\xi^2}{c^2} \right]^{1/2}. \quad (5)$$

Below we also use the dimensionless variable $y = 2k_{\perp}a$ instead of k_{\perp} .

We begin from the consideration of the Casimir interaction between two parallel dielectric films in vacuum. In this case $\varepsilon^{(\pm 2)}(\omega) = 1$, $k^{(n)}(0, k_{\perp}) = k_{\perp}$ and from Eq. (4) using Eq. (5) one obtains $r_{\text{TE}}^{(n,n')}(0, k_{\perp}) = 0$ and following nonzero TM reflection coefficients

$$r_{\text{TM}}^{(0,\pm 1)}(0, k_{\perp}) = -r_{\text{TM}}^{(\pm 1,\pm 2)}(0, k_{\perp}) = \frac{\varepsilon_0^{(\pm 1)} - 1}{\varepsilon_0^{(\pm 1)} + 1} \equiv r_0^{(\pm 1)}, \quad (6)$$

where $\varepsilon_0^{(n)} \equiv \varepsilon^{(n)}(0)$. Then for the reflection coefficients (3) we arrive at

$$\begin{aligned} R_{\text{TM}}^{(\pm)}(0, k_{\perp}) &= r_0^{(\pm 1)} \frac{1 - e^{-2k_{\perp}d_{\pm}}}{1 - r_0^{(\pm 1)2} e^{-2k_{\perp}d_{\pm}}}, \\ R_{\text{TE}}^{(\pm)}(0, k_{\perp}) &= 0. \end{aligned} \quad (7)$$

In all subsequent calculations we assume that our films are thin as compared to separation distance, i.e., $d_{\pm} \ll a$.

Now we rewrite the integral in Eq. (2) in terms of the variable y and expand the quantities $R_{\text{TM}}^{(\pm)}(0, y)$ in powers of a small parameter d_{\pm}/a preserving only the main contribution

$$R_{\text{TM}}^{(\pm)}(0, y) = r_0^{(\pm 1)} \frac{y}{1 - r_0^{(\pm 1)2}} \frac{d_{\pm}}{a} + O\left(\frac{d_{\pm}^2}{a^2}\right). \quad (8)$$

Substituting Eq. (8) in Eq. (2), one obtains

$$\mathcal{F}(a, T) \approx \frac{k_B T}{16\pi a^2} \int_0^{\infty} y dy \ln \left[1 - \frac{r_0^{(1)} r_0^{(-1)} d_+ d_-}{(1 - r_0^{(1)2})(1 - r_0^{(-1)2}) a^2} y^2 e^{-y} \right]. \quad (9)$$

Expanding the logarithm in Eq. (9) in powers of a small parameter $d_+ d_- / a^2$ and integrating, we finally obtain

$$\mathcal{F}(a, T) \approx - \frac{3r_0^{(1)} r_0^{(-1)}}{8\pi(1 - r_0^{(1)2})(1 - r_0^{(-1)2})} \frac{k_B T d_+ d_-}{a^4} \quad (10)$$

or, for two similar films with $d_+ = d_- = d$ and $r_0^{(1)} = r_0^{(-1)} \equiv r_0$

$$\mathcal{F}(a, T) \approx -\frac{3r_0^2}{8\pi(1-r_0^2)^2} \frac{k_B T d^2}{a^4}. \quad (11)$$

This result demonstrates the classical limit, but an unusually rapid decrease with the increase of separation (the inverse fourth power instead of the inverse second) if to compare with the classical limit for the case of two dielectric semispaces. The physical reason for this difference is explained by the presence of two additional dimensional parameters d_{\pm} and will be further discussed in Sec. V in connection with the case of graphene sheets. From Eq. (10) for the Casimir pressure one finds

$$P(a, T) \approx -\frac{3r_0^{(1)}r_0^{(-1)}}{2\pi(1-r_0^{(1)2})(1-r_0^{(-1)2})} \frac{k_B T d_+ d_-}{a^5}. \quad (12)$$

Now we consider the Casimir interaction of a thin dielectric film with a dielectric semispace. In this case $\varepsilon^{(2)}(\omega) = 1$, $\varepsilon^{(-2)}(\omega) = \varepsilon^{(-1)}(\omega)$ and, again, $k^{(n)}(0, k_{\perp}) = k_{\perp}$. Thus, from Eqs. (3) and (4), $r_{\text{TE}}^{(n, n')}(0, k_{\perp}) = R_{\text{TE}}^{(\pm)}(0, k_{\perp}) = 0$. For the TM reflection coefficients we obtain

$$\begin{aligned} r_{\text{TM}}^{(0,1)}(0, k_{\perp}) &= r_0^{(1)}, & r_{\text{TM}}^{(1,2)}(0, k_{\perp}) &= -r_0^{(1)}, \\ r_{\text{TM}}^{(0,-1)}(0, k_{\perp}) &= \frac{\varepsilon_0^{(-2)} - 1}{\varepsilon_0^{(-2)} + 1} \equiv r_0^{(-2)}, \\ r_{\text{TM}}^{(-1,-2)}(0, k_{\perp}) &= 0, & R_{\text{TM}}^{(-)}(0, k_{\perp}) &= r_0^{(-2)}, \\ R_{\text{TM}}^{(+)}(0, k_{\perp}) &= r_0^{(1)} \frac{1 - e^{-2k_{\perp}d_+}}{1 - r_0^{(1)2} e^{-2k_{\perp}d_+}}. \end{aligned} \quad (13)$$

Expanding, as above, in powers of a small parameter d_+/a and using the variable y , we obtain from Eq. (2)

$$\mathcal{F}(a, T) \approx \frac{k_B T}{16\pi a^2} \int_0^{\infty} y dy \ln \left[1 - \frac{r_0^{(1)} r_0^{(-2)} d_+}{(1 - r_0^{(1)2}) a} y e^{-y} \right]. \quad (14)$$

After expansion of the logarithm in powers of the same parameter one arrives at

$$\begin{aligned} \mathcal{F}(a, T) &\approx -\frac{r_0^{(1)} r_0^{(-2)}}{8\pi(1-r_0^{(1)2})} \frac{k_B T d_+}{a^3}, \\ P(a, T) &\approx -\frac{3r_0^{(1)} r_0^{(-2)}}{8\pi(1-r_0^{(1)2})} \frac{k_B T d_+}{a^4}. \end{aligned} \quad (15)$$

These results again demonstrate the classical limit with some specific dependence on separation caused by the fact that one of the semispaces was replaced with a thin film (the comparison with the case of a graphene sheet interacting with a dielectric plate is contained in Sec. V).

Next we deal with the classical Casimir interaction between the same dielectric film and a metallic semispace. In this case, again, $\varepsilon^{(2)}(\omega) = 1$, $\varepsilon^{(-2)}(\omega) = \varepsilon^{(-1)}(\omega)$ and $k^{(1)}(0, k_\perp) = k^{(2)}(0, k_\perp) = k_\perp$. Thus, from Eqs. (3) and (4), we have $r_{\text{TE}}^{(n,n')}(0, k_\perp) = R_{\text{TE}}^{(+)}(0, k_\perp) = 0$, where n and n' here take the values 0, 1, 2 and also $n = -1$, $n' = -2$. Note that the value of the coefficient $r_{\text{TE}}^{(0,-1)}(0, k_\perp) = r_{\text{TE}}^{(0,-2)}(0, k_\perp)$ depends on the used model of metal (see below) and can be not equal to zero leading to a nonzero value of $R_{\text{TE}}^{(-)}(0, k_\perp)$. This, however, does not influence on the result due to Eq. (2). For the TM reflection coefficient $R_{\text{TM}}^{(+)}(0, k_\perp)$ we obtain the result already presented in Eq. (13). As to $R_{\text{TM}}^{(-)}(0, k_\perp)$, it is easily calculated taking into account that for any model of the dielectric permittivity of a metal $|\varepsilon^{(-2)}(\omega)| \rightarrow \infty$ when $\omega \rightarrow 0$ leading to

$$r_{\text{TM}}^{(0,-1)}(0, k_\perp) = R_{\text{TM}}^{(-)}(0, k_\perp) = 1. \quad (16)$$

Thus, the Casimir free energy per unit area after an expansion in small parameter d_+/a takes the form

$$\mathcal{F}(a, T) \approx \frac{k_B T}{16\pi a^2} \int_0^\infty y dy \ln \left[1 - \frac{r_0^{(1)} d_+}{(1 - r_0^{(1)2}) a} y e^{-y} \right] \quad (17)$$

resulting in

$$\begin{aligned} \mathcal{F}(a, T) &\approx -\frac{r_0^{(1)}}{8\pi(1 - r_0^{(1)2})} \frac{k_B T d_+}{a^3}, \\ P(a, T) &\approx -\frac{3r_0^{(1)}}{8\pi(1 - r_0^{(1)2})} \frac{k_B T d_+}{a^4}. \end{aligned} \quad (18)$$

This can be also obtained from Eq. (15) in the limiting case $r_0^{(-2)} \rightarrow 1$, as it should be when the dielectric plate is replaced by a metallic.

III. INTERACTION BETWEEN TWO METALLIC FILMS

We now turn our attention to the case of two parallel metallic films. As discussed above, in this case $|\varepsilon^{(\pm 1)}(\omega)| \rightarrow \infty$ when $\omega \rightarrow 0$. The low-frequency behavior of metals is commonly

described by the Drude dielectric function

$$\varepsilon_D^{(\pm 1)}(\omega) = 1 - \frac{\omega_{p,\pm 1}^2}{\omega[\omega + i\gamma_{\pm 1}(T)]}, \quad (19)$$

where $\omega_{p,\pm 1}$ are the plasma frequencies and $\gamma_{\pm 1}(T)$ are the relaxation parameters for the upper and lower films, respectively. At sufficiently low frequencies it holds $\omega \ll \gamma_{\pm 1}(T)$ and Eq. (19) results in $\varepsilon_D^{(\pm 1)}(\omega) \sim \omega^{-1}$, as it should be at quasistatic ω in accordance to the Maxwell equations. It was demonstrated, however, in several experiments with metallic test bodies^{38–42} that theoretical predictions of the Lifshitz theory using Eq. (19) are excluded by the measurement data. The data were found in excellent agreement with the low-frequency behavior given by the plasma model

$$\varepsilon_p^{(\pm 1)}(\omega) = 1 - \frac{\omega_{p,\pm 1}^2}{\omega^2}. \quad (20)$$

This model is in fact justified in the frequency region of infrared optics $\omega \gg \gamma_{\pm 1}(T)$ where the relaxation properties do not play any role. What is more, the Lifshitz theory using Eq. (19) was shown^{43–45} to violate the Nernst heat theorem whereas the same theory is thermodynamically consistent when using Eq. (20). (We note that in two other experiments^{46,47} the Lifshitz theory using Eq. (19) was confirmed, but these experiments are not direct measurements of the Casimir force and their results were disputed in the literature.^{48–52}) Keeping in mind that the fundamental reasons behind preference of the dielectric permittivity (20) in the equilibrium fluctuational electrodynamics remain unclear, below we perform all calculations using both Eqs. (19) and (20) when the result is sensitive to the low-frequency behavior of ε .

First, we consider the two films described at low frequencies by the Drude model (19). In this case it holds

$$\lim_{\xi \rightarrow 0} \varepsilon^{(n)}(i\xi)\xi^2 = 0 \quad (21)$$

and $k^{(n)}(0, k_{\perp}) = k_{\perp}$. As a result, from Eqs. (3) and (4) one obtains

$$r_{\text{TE}}^{(n,n')}(0, k_{\perp}) = R_{\text{TE}}^{(\pm)}(0, k_{\perp}) = 0 \quad (22)$$

and for the TM mode

$$r_{\text{TM}}^{(0,\pm 1)}(0, k_{\perp}) = -r_{\text{TM}}^{(\pm 1,\pm 2)}(0, k_{\perp}) = R_{\text{TM}}^{(\pm)}(0, k_{\perp}) = 1. \quad (23)$$

Substituting Eqs. (22) and (23) in Eq. (2) written in terms of the variable y , we find the Casimir free energy per unit area calculated using the Drude model

$$\begin{aligned}\mathcal{F}_D(a, T) &= \frac{k_B T}{16\pi a^2} \int_0^\infty y dy \ln(1 - e^{-y}) \\ &= -\frac{k_B T \zeta(3)}{16\pi a^2},\end{aligned}\quad (24)$$

where $\zeta(z)$ is the Riemann zeta function. Note that the result (24) does not depend on the film thicknesses and coincides with respective result for two metallic semispaces described by the Drude model.² In the high-temperature limit the same result was also obtained³⁶ for atomically thin Au films described by the anisotropic dielectric functions.

Now we consider the two films described at low frequencies by the plasma dielectric function. This case is more interesting and presents several possibilities depending on the values of involved parameters. Concerning the TM mode, the result in Eq. (23) and, thus, in Eq. (24) remains valid. However, instead of Eq. (21), for the plasma model we have

$$\lim_{\xi \rightarrow 0} \varepsilon^{(\pm 1)}(i\xi) \xi^2 = \omega_{p, \pm 1}^2, \quad (25)$$

and this leads to a nonzero contribution of the TE mode. From Eqs. (3)–(5) one obtains

$$\begin{aligned}r_{\text{TE}}^{(0, \pm 1)}(0, k_\perp) &= -r_{\text{TE}}^{(\pm 1, \pm 2)}(0, k_\perp) \\ &= \frac{k_\perp - (k_\perp^2 + \omega_{p, \pm 1}^2/c^2)^{1/2}}{k_\perp + (k_\perp^2 + \omega_{p, \pm 1}^2/c^2)^{1/2}} \equiv r_{\text{TE}, p}^{(\pm 1)}(k_\perp), \\ R_{\text{TE}}^{(\pm)}(0, k_\perp) &= \frac{r_{\text{TE}, p}^{(\pm 1)}(k_\perp) \{1 - \exp[-2(k_\perp^2 + \omega_{p, \pm 1}^2/c^2)^{1/2} d_\pm]\}}{1 - r_{\text{TE}, p}^{(\pm 1)2}(k_\perp) \exp[-2(k_\perp^2 + \omega_{p, \pm 1}^2/c^2)^{1/2} d_\pm]}.\end{aligned}\quad (26)$$

It is convenient to express the last reflection coefficient in terms of the variable y

$$R_{\text{TE}}^{(\pm)}(0, y) = \frac{r_{\text{TE}, p}^{(\pm 1)}(y) \{1 - \exp[-d_\pm(y^2 + \tilde{\omega}_{p, \pm 1}^2)^{1/2}/a]\}}{1 - r_{\text{TE}, p}^{(\pm 1)2}(y) \exp[-d_\pm(y^2 + \tilde{\omega}_{p, \pm 1}^2)^{1/2}/a]}, \quad (27)$$

where $\tilde{\omega}_{p, \pm 1} = 2a\omega_{p, \pm 1}/c$ and

$$r_{\text{TE}, p}^{(\pm 1)}(y) = \frac{y - \sqrt{y^2 + \tilde{\omega}_{p, \pm 1}^2}}{y + \sqrt{y^2 + \tilde{\omega}_{p, \pm 1}^2}}. \quad (28)$$

Furthermore, we introduce the penetration depth of the electromagnetic oscillations into metals of films $\delta_{\pm 1} = c/\omega_{p, \pm 1}$ (it is equal to approximately 22 nm for Au). It is assumed that

$\delta_{\pm 1} \ll a$, so that the parameter $\beta_{\pm 1} = \delta_{\pm 1}/(2a) \ll 1$. Expressing Eq. (27) in terms of the quantities $\beta_{\pm 1}$ and $\delta_{\pm 1}$ and expanding in powers of $\beta_{\pm 1}$, we arrive at

$$R_{\text{TE}}^{(\pm)}(0, y) \approx \frac{(-1 + 2\beta_{\pm 1}y)[1 - \exp(-2d_{\pm}/\delta_{\pm 1})]}{1 - \exp(-2d_{\pm}/\delta_{\pm 1}) + 4\beta_{\pm 1}y \exp(-2d_{\pm}/\delta_{\pm 1})}. \quad (29)$$

The following calculations depend on the values of our parameters. For sufficiently thick films satisfying the condition

$$\frac{d_{\pm}}{\delta_{\pm 1}} \gg 2\beta_{\pm 1} = \frac{\delta_{\pm 1}}{a} \quad (30)$$

one can expand the right-hand side of Eq. (29) in powers of a small parameter $\delta_{\pm 1}/a$ and obtain

$$R_{\text{TE}}^{(\pm)}(0, y) \approx -1 + 2\beta_{\pm 1}y \coth \frac{d_{\pm}}{\delta_{\pm 1}}. \quad (31)$$

Note that Eq. (30) is satisfied also for films of any thickness if the separation distance a is sufficiently large. By contrast, for very thin films satisfying the condition

$$\frac{d_{\pm}}{\delta_{\pm 1}} \ll \frac{\delta_{\pm 1}}{a} \ll 1, \quad (32)$$

one can expand the exponents in Eq. (29) in powers of $d_{\pm}/\delta_{\pm 1}$. This leads to the result

$$R_{\text{TE}}^{(\pm)}(0, y) \approx -\frac{d_{\pm}/\delta_{\pm 1}}{d_{\pm}/\delta_{\pm 1} + 2\beta_{\pm 1}y}. \quad (33)$$

If both films satisfy Eq. (30) one finds from Eq. (31)

$$R_{\text{TE}}^{(+)}(0, y)R_{\text{TE}}^{(-)}(0, y) \approx 1 - 2\beta_1y \coth \frac{d_+}{\delta_1} - 2\beta_{-1}y \coth \frac{d_-}{\delta_{-1}}. \quad (34)$$

Substituting Eq. (34) in Eq. (2) written in terms of the variable y and performing integration in y , we obtain for the TE contribution to the Casimir free energy

$$\mathcal{F}_{\text{TE}}(a, T) \approx -\frac{k_B T \zeta(3)}{16\pi a^2} \left[1 - 2 \left(\frac{\delta_1}{a} \coth \frac{d_+}{\delta_1} + \frac{\delta_{-1}}{a} \coth \frac{d_-}{\delta_{-1}} \right) \right]. \quad (35)$$

The contribution of the TM mode to the free energy is given by Eq. (24). Then the total Casimir free energy per unit area in the classical limit is given by

$$\mathcal{F}_p(a, T) \approx -\frac{k_B T \zeta(3)}{8\pi a^2} \left[1 - \frac{\delta_1}{a} \coth \frac{d_+}{\delta_1} - \frac{\delta_{-1}}{a} \coth \frac{d_-}{\delta_{-1}} \right]. \quad (36)$$

Here the magnitude of the main contribution is twice that in Eq. (24) and our result depends on the film properties.

Let now the lower film satisfies Eq. (30) and the upper film satisfies Eq. (32). In this case using Eqs. (31) and (33) in the leading order we obtain

$$R_{\text{TE}}^{(+)}(0, y)R_{\text{TE}}^{(-)}(0, y) \approx -\frac{d_+/\delta_1}{d_+/\delta_1 + 2\beta_1 y}. \quad (37)$$

Then, expanding the logarithm under the integral in Eq. (2) and integrating using Eq. (37) one arrives at the result

$$\mathcal{F}_{\text{TE}}(a, T) \approx -\frac{k_B T d_+}{16\pi a \delta_1^2} \left[1 - \frac{d_+ a}{\delta_1^2} e^{d_+ a/\delta_1^2} \Gamma\left(0, \frac{d_+ a}{\delta_1^2}\right) \right], \quad (38)$$

where $\Gamma(x, y)$ is the incomplete gamma function. Note that due to Eq. (32) the correction to unity on the right-hand side of Eq. (38) is negligibly small. By adding the contribution of the TM mode, one arrives to the total Casimir free energy per unit area

$$\mathcal{F}_p(a, T) \approx -\frac{k_B T \zeta(3)}{16\pi a^2} \left[1 + \frac{d_+ a}{\zeta(3) \delta_1^2} \right]. \quad (39)$$

Finally we consider the two films satisfying Eq. (32). In this case from Eq. (33) we have

$$R_{\text{TE}}^{(+)}(0, y)R_{\text{TE}}^{(-)}(0, y) \approx \frac{d_+ d_-}{\delta_1^2 \delta_{-1}^2} \frac{a^2}{(d_+ a/\delta_1^2 + y)(d_- a/\delta_{-1}^2 + y)}. \quad (40)$$

After integration according to Eq. (2), one obtains

$$\begin{aligned} \mathcal{F}_{\text{TE}}(a, T) &\approx -\frac{k_B T}{16\pi} \frac{d_+ d_-}{d_- \delta_1^2 - d_+ \delta_{-1}^2} \\ &\times \left[\frac{d_-}{\delta_{-1}^2} e^{d_- a/\delta_{-1}^2} \Gamma\left(0, \frac{d_- a}{\delta_{-1}^2}\right) - \frac{d_+}{\delta_1^2} e^{d_+ a/\delta_1^2} \Gamma\left(0, \frac{d_+ a}{\delta_1^2}\right) \right]. \end{aligned} \quad (41)$$

The total free energy is obtained by adding Eq. (24) to this equation. It is seen that the contribution of the TE mode is much smaller than the contribution of the TM mode given by Eq. (24). The respective results for the Casimir pressure are obtained from Eqs. (24), (36), (39) and (41) by the negative differentiation with respect to a .

Note that the free energy \mathcal{F}_p in all cases considered depends on film thicknesses, as opposed to \mathcal{F}_D obtained using the Drude model. This is because the classical limit for the Drude metals does not depend on any metallic property due to $r_{\text{TM}}(0, k_\perp) = 1$ and $r_{\text{TE}}(0, k_\perp) = 0$. As to the plasma model, $r_{\text{TE}}(0, k_\perp) \neq 0$ and depends on the penetration depth of electromagnetic oscillations into the metal. Then it is not surprising that, under different relationships among the penetration depths and film thicknesses, different classical limits considered above are possible which depend on both the penetration depths and film thicknesses.

IV. FILMS DEPOSITED ON SUBSTRATES

In this section we consider the classical Casimir interaction of a thin film deposited on a substrate with thick plates (semispaces) made of different materials or with another thin film also deposited on a substrate. We begin from the case of a dielectric film having the dielectric permittivity $\varepsilon^{(1)}(\omega)$ deposited on a dielectric semispace having the dielectric permittivity $\varepsilon^{(2)}(\omega)$ interacting with a dielectric semispace having the dielectric permittivity $\varepsilon^{(-1)}(\omega) = \varepsilon^{(-2)}(\omega)$ (see Fig. 1). Then from Eqs. (3)–(5) we obtain

$$\begin{aligned} R_{\text{TE}}^{(\pm)}(0, k_{\perp}) &= 0, & r_{\text{TM}}^{(1,2)}(0, k_{\perp}) &= \frac{\varepsilon_0^{(2)} - \varepsilon_0^{(1)}}{\varepsilon_0^{(2)} + \varepsilon_0^{(1)}} \equiv r_0^{(2,1)}, \\ r_{\text{TM}}^{(-1,-2)}(0, k_{\perp}) &= 0, & r_{\text{TM}}^{(0,\pm 1)}(0, k_{\perp}) &= r_0^{(\pm 1)}, \\ R_{\text{TM}}^{(+)}(0, k_{\perp}) &= \frac{r_0^{(1)} + r_0^{(2,1)} e^{-2k_{\perp} d_+}}{1 + r_0^{(1)} r_0^{(2,1)} e^{-2k_{\perp} d_+}} & R_{\text{TM}}^{(-)}(0, k_{\perp}) &= r_0^{(-1)}. \end{aligned} \quad (42)$$

Substituting Eq. (42) in Eq. (2), using the variable y and expanding in powers of a small parameter d_+/a under the integral one finds

$$\begin{aligned} \mathcal{F}(a, T) &\approx \frac{k_B T}{16\pi a^2} \int_0^{\infty} y dy \ln \left\{ 1 - r_0^{(-1)} \right. \\ &\quad \left. \times \left[r_0^{(2)} - \frac{d_+}{a} \frac{\varepsilon_0^{(2)^2} - \varepsilon_0^{(1)^2}}{\varepsilon_0^{(1)} (1 + \varepsilon_0^{(2)})^2} y \right] e^{-y} \right\}, \end{aligned} \quad (43)$$

where $r_0^{(2)}$ is defined in the same way as $r_0^{(-2)}$ in Eq. (13). Integration in Eq. (43) leads to

$$\mathcal{F}(a, T) \approx \frac{k_B T \text{Li}_3(r_0^{(-1)} r_0^{(2)})}{16\pi a^2} \left[1 - 2 \frac{\varepsilon_0^{(2)^2} - \varepsilon_0^{(1)^2}}{\varepsilon_0^{(1)} (\varepsilon_0^{(2)} - 1)} \frac{d_+}{a} \right], \quad (44)$$

where $\text{Li}_n(z)$ is the polylogarithm function.

In a similar way one can find the Casimir free energy for a dielectric film deposited on thick dielectric plate and interacting with a metallic semispace. Here the contribution of the TE mode is again equal to zero due to $R_{\text{TE}}^{(+)}(0, k_{\perp}) = 0$ and $R_{\text{TM}}^{(-)}(0, k_{\perp}) = 1$. As a result,

$$\mathcal{F}(a, T) \approx -\frac{k_B T \text{Li}_3(r_0^{(2)})}{16\pi a^2} \left[1 - 2 \frac{\varepsilon_0^{(2)^2} - \varepsilon_0^{(1)^2}}{\varepsilon_0^{(1)} (\varepsilon_0^{(2)} - 1)} \frac{d_+}{a} \right] \quad (45)$$

independently of the model of a metal used.

The next case to consider is the dielectric film deposited on a metallic plate and interacting with a dielectric plate. The TE mode, again, does not contribute, this time due to

$R_{\text{TE}}^{(-)}(0, k_{\perp}) = 0$, and the result does not depend on a model of metal. From Eqs. (3)–(5) one finds

$$R_{\text{TM}}^{(+)}(0, k_{\perp}) = \frac{r_0^{(1)} + e^{-2k_{\perp}d_+}}{1 + r_0^{(1)}e^{-2k_{\perp}d_+}}, \quad R_{\text{TM}}^{(-)}(0, k_{\perp}) = r_0^{(-1)}. \quad (46)$$

Substituting this in Eq. (2), using the variable y and expanding in powers of d_+/a , we obtain

$$\begin{aligned} \mathcal{F}(a, T) &\approx \frac{k_B T}{16\pi a^2} \int_0^{\infty} y dy \\ &\times \left[\ln(1 - r_0^{(-1)} e^{-y}) + \frac{r_0^{(-1)}}{\varepsilon_0^{(1)}} \frac{d_+}{a} \frac{y}{e^y - r_0^{(-1)}} \right]. \end{aligned} \quad (47)$$

After the integration of Eq. (47) one arrives at

$$\mathcal{F}(a, T) \approx -\frac{k_B T \text{Li}_3(r_0^{(-1)})}{16\pi a^2} \left[1 - \frac{2}{\varepsilon_0^{(1)}} \frac{d_+}{a} \right]. \quad (48)$$

The case of a dielectric film deposited on a metallic plate and interacting with a metallic plate is a bit more complicated. Here, the result depends on the model of metal. If the low-frequency behavior of $\varepsilon^{(2)}(\omega)$ and $\varepsilon^{(-1)}(\omega) = \varepsilon^{(-2)}(\omega)$ is described by the Drude model, we have $R_{\text{TE}}^{(-)}(0, k_{\perp}) = 0$ and $r_0^{(-1)} = 1$. Then, repeating all calculations, as in the previous case, one finds

$$\mathcal{F}_D(a, T) \approx -\frac{k_B T \zeta(3)}{16\pi a^2} \left[1 - \frac{2}{\varepsilon_0^{(1)}} \frac{d_+}{a} \right]. \quad (49)$$

Taking into account that $\text{Li}_3(1) = \zeta(3)$, this is in agreement with Eq. (48).

Now we admit that the low-frequency behavior of $\varepsilon^{(2)}(\omega)$ and $\varepsilon^{(-1)}(\omega) = \varepsilon^{(-2)}(\omega)$ is described by the plasma model. In this case the contribution of the TM mode remains unchanged, i.e., it is given by Eq. (49). In addition, the contribution of the TE mode becomes nonzero

$$\begin{aligned} R_{\text{TE}}^{(+)}(0, k_{\perp}) &= \frac{k_{\perp} - (k_{\perp}^2 + \omega_{p,2}^2/c^2)^{1/2}}{k_{\perp} + (k_{\perp}^2 + \omega_{p,2}^2/c^2)^{1/2}} e^{-2k_{\perp}d_+}, \\ R_{\text{TE}}^{(-)}(0, k_{\perp}) &= r_{\text{TE},p}^{(-1)}(k_{\perp}), \end{aligned} \quad (50)$$

where $r_{\text{TE},p}^{(-1)}(k_{\perp})$ is defined in Eq. (26) and $\omega_{p,2}$ is the plasma frequency of the substrate metal. Using the variable y and performing the expansion in powers of d_+/a , we obtain

$$\begin{aligned} R_{\text{TE}}^{(+)}(0, k_{\perp}) &\approx -1 + 2\beta_2 y + \frac{d_+}{a} y, \\ R_{\text{TE}}^{(-)}(0, k_{\perp}) &\approx -1 + 2\beta_{-1} y, \end{aligned} \quad (51)$$

where $\beta_2 \equiv \delta_2/(2a)$, $\delta_2 = c/\omega_{p,2}$ and β_{-1} is defined in Sec. III. Using Eqs. (2) and (51), to the first order of small parameters β_{-1} , β_2 and d_+/a , for the contribution of the TE mode to the Casimir free energy we have

$$\mathcal{F}_{\text{TE}}(a, T) \approx \frac{k_B T}{16\pi a^2} \int_0^\infty y dy \times \ln \left\{ 1 - \left[1 - 2(\beta_2 + \beta_{-1})y - \frac{d_+}{a}y \right] e^{-y} \right\}. \quad (52)$$

Expanding the logarithm in powers of the same small parameters and integrating, we obtain

$$\mathcal{F}_{\text{TE}}(a, T) \approx \frac{k_B T \zeta(3)}{16\pi a^2} \left[-1 + 4(\beta_2 + \beta_{-1}) + 2\frac{d_+}{a} \right]. \quad (53)$$

By adding to this equation the contribution of the TM mode in Eq. (49), the final result is

$$\mathcal{F}_p(a, T) \approx -\frac{k_B T \zeta(3)}{8\pi a^2} \left[1 - \frac{\delta_2 + \delta_{-1}}{a} - \frac{\varepsilon_0^{(1)} + 1}{\varepsilon_0^{(1)}} \frac{d_+}{a} \right]. \quad (54)$$

Thus, in the case of the plasma metals, the magnitude of the main contribution is larger by a factor of 2, as compared to Eq. (49), and the correction term depends on the penetration depth of electromagnetic oscillations into a metal.

Now we consider the classical Casimir interaction of two thin films each of which is deposited on a thick plate (semispace). We begin with two dielectric films with dielectric permittivities $\varepsilon^{(\pm 1)}$ deposited on the dielectric semispaces having the permittivities $\varepsilon^{(\pm 2)}$, respectively. Calculations for this case are presented in Appendix A. Substituting Eq. (A3) in Eq. (2), expanding the logarithm and performing the integration, one arrives at

$$\mathcal{F}(a, T) \approx -\frac{k_B T \text{Li}_3(r_0^{(2)} r_0^{(-2)})}{16\pi a^2} \times \left\{ 1 - 2\frac{\varepsilon_0^{(2)^2} - \varepsilon_0^{(1)^2}}{\varepsilon_0^{(1)}[\varepsilon_0^{(2)^2} - 1]} \frac{d_+}{a} - 2\frac{\varepsilon_0^{(-2)^2} - \varepsilon_0^{(-1)^2}}{\varepsilon_0^{(-1)}[\varepsilon_0^{(-2)^2} - 1]} \frac{d_-}{a} \right\}. \quad (55)$$

If we now replace the lower dielectric plate (semispace) with a metallic one, the free energy of the Casimir interaction between two dielectric films does not depend on the model of a metal used. Similar to the respective case in Sec. III, the result can be obtained from Eq. (55) in the limiting case $\varepsilon_0^{(-2)^2} \rightarrow \infty$:

$$\mathcal{F}(a, T) \approx -\frac{k_B T \text{Li}_3(r_0^{(2)})}{16\pi a^2} \times \left\{ 1 - 2\frac{\varepsilon_0^{(2)^2} - \varepsilon_0^{(1)^2}}{\varepsilon_0^{(1)}[\varepsilon_0^{(2)^2} - 1]} \frac{d_+}{a} - 2\frac{2}{\varepsilon_0^{(-1)}} \frac{d_-}{a} \right\}. \quad (56)$$

The case when both dielectric films are deposited on the metallic semispaces is a bit more cumbersome. Here the result depends on the model of a metal. If the Drude model (19) is used, one has

$$R_{\text{TE}}^{(\pm)}(0, y) = 0, \quad R_{\text{TM}}^{(\pm)}(0, y) \approx 1 - \frac{1}{\varepsilon_0^{(\pm 1)}} \frac{d_{\pm}}{a} y. \quad (57)$$

From this it follows:

$$R_{\text{TM}}^{(+)}(0, y) R_{\text{TM}}^{(-)}(0, y) \approx 1 - \frac{1}{\varepsilon_0^{(1)}} \frac{d_+}{a} y - \frac{1}{\varepsilon_0^{(-1)}} \frac{d_-}{a} y \quad (58)$$

and from Eq. (2)

$$\mathcal{F}_D(a, T) \approx -\frac{k_B T \zeta(3)}{16\pi a^2} \left[1 - \frac{2}{\varepsilon_0^{(1)}} \frac{d_+}{a} - \frac{2}{\varepsilon_0^{(-1)}} \frac{d_-}{a} \right]. \quad (59)$$

If the metal of semispaces is described by the plasma model (20), the reflection coefficients $R_{\text{TE}}^{(\pm)}(0, y)$ become nonzero. Calculation details for this case are given in Appendix A. By adding the contribution of the TM mode [which is the same as in Eq. (59)] to the contribution of the TE mode presented in Eq. (A6), we obtain

$$\mathcal{F}_p(a, T) \approx -\frac{k_B T \zeta(3)}{8\pi a^2} \left(1 - \frac{\delta_2 + \delta_{-2}}{a} - \frac{\varepsilon_0^{(1)} + 1}{\varepsilon_0^{(1)}} \frac{d_+}{a} - \frac{\varepsilon_0^{(-1)} + 1}{\varepsilon_0^{(-1)}} \frac{d_-}{a} \right). \quad (60)$$

The Casimir pressures for all cases considered in this section can be easily obtained from Eqs. (44), (45), (48), (49), (54)–(56), (59), and (60) by the differentiation with respect to a . Note also that the case of two metallic films covering semispaces made of any material is equivalent to two metallic semispaces if the films are sufficiently thick. Because of this we do not consider it here.

V. APPLICATIONS TO THE CASIMIR INTERACTION OF TWO GRAPHENE SHEETS

As mentioned in Sec. II, for two films described by the dielectric permittivity the classical regime holds for separations larger than a few micrometers. For two sheets of pristine graphene described by the polarization tensor in the framework of Dirac model the classical regime starts at much shorter separations.²² In this regime the free energy of the Casimir interaction per unit area of graphene sheet is again given by Eq. (2) where the reflection

coefficients $R_\alpha^{(+)}(0, k_\perp) = R_\alpha^{(-)}(0, k_\perp) \equiv R_\alpha(0, k_\perp)$ take the form^{23,31}

$$\begin{aligned} R_{\text{TM}}(0, k_\perp) &= \frac{\Pi_{00}(0, k_\perp)}{\Pi_{00}(0, k_\perp) + 2\hbar k_\perp}, \\ R_{\text{TE}}(0, k_\perp) &= -\frac{\Pi_{\text{tr}}(0, k_\perp) - \Pi_{00}(0, k_\perp)}{\Pi_{\text{tr}}(0, k_\perp) - \Pi_{00}(0, k_\perp) + 2\hbar k_\perp}. \end{aligned} \quad (61)$$

Here, Π_{00} is the 00-component of the polarization tensor in (2+1)-dimensional space-time and trace stands for the sum of spatial components Π_1^1 and Π_2^2 all taken at zero frequency.

The explicit expressions are:^{23,30,31,53}

$$\begin{aligned} \Pi_{00}(0, k_\perp) &= \frac{16\alpha k_B T c}{v_F^2} \int_0^1 dx \ln[2 \cosh \varphi(k_\perp, x)], \\ \Pi_{\text{tr}}(0, k_\perp) &= \Pi_{00}(0, k_\perp) + \frac{8\alpha \hbar v_F k_\perp}{c} \int_0^1 dx \sqrt{x(1-x)} \tanh \varphi(k_\perp, x), \end{aligned} \quad (62)$$

where

$$\varphi(k_\perp, x) = \frac{\hbar v_F k_\perp}{2k_B T} \sqrt{x(1-x)}, \quad (63)$$

$\alpha = e^2/(\hbar c)$ is the fine structure constant and $v_F \approx c/300$ is the Fermi velocity.

Substituting Eq. (61) in Eq. (2), one arrives to the Casimir free energy per unit area and pressure between two sheets of gapless graphene in the classical limit^{22,23,31}

$$\begin{aligned} \mathcal{F}(a, T) &\approx -\frac{k_B T \zeta(3)}{16\pi a^2} \left[1 - \frac{1}{4\alpha \ln 2} \left(\frac{v_F}{c} \right)^2 \frac{\hbar c}{a k_B T} \right], \\ P(a, T) &\approx -\frac{k_B T \zeta(3)}{8\pi a^3} \left[1 - \frac{3}{8\alpha \ln 2} \left(\frac{v_F}{c} \right)^2 \frac{\hbar c}{a k_B T} \right]. \end{aligned} \quad (64)$$

Numerical computations show that the asymptotic expressions (64) are applicable at much smaller separations than the asymptotic expressions obtained in Secs. II–IV for usual dielectric and metallic films. Thus, at $T = 300$ K the pressure values calculated using Eq. (64) agree in the limits of 1% and 5% with the total pressure computed by taking into account the contributions from all Matsubara frequencies at separations $a > 370$ nm and $a > 150$ nm, respectively. Note that the dependence of the free energy on separation proportional to a^{-2} was also obtained in Refs.^{22,28} and⁵⁴.

The main, first, term on the right-hand side of Eq. (64) does not contain the Planck constant and, thus, corresponds to the classical limit.³⁷ We emphasize that for two dielectric films with no free charge carriers the classical limit for the free energy in Eqs. (10) and (11) contains the thicknesses of the films and is inversely proportional to the fourth power of separation. For this reason, if graphene sheets are modeled as two insulator films (see,

e.g., Refs.^{27,55}), the computed free energy deviates significantly from that computed using the polarization tensor within a wide region of separations. It was hypothesized^{27,55} that the account of thermally excited charge carriers at nonzero temperature (which are always present in dielectric material in the form of dc conductivity) should change the long-distance power $n = 4$ as in Eqs. (10) and (11), to $n = 2$, as in Eq. (64).

In fact the dc conductivity of dielectrics can be described by the Drude-type additional term in the dielectric permittivity which leads to Eq. (21) and then to Eqs. (22) and (23). As a result, the free energy of two dielectric films with account of dc conductivity, as well as of two metallic films described by the Drude model, is given by Eq. (24). This is in agreement with the main, first, term on the right-hand side of Eq. (64) and does not depend on the film thicknesses. Thus, the description of a gapless graphene at nonzero temperature as a dielectric film possessing some dc conductivity is really a better model leading to a correct classical limit. It should be noted, however, that for dielectric films with account of dc conductivity the asymptotic regime (24) is achieved starting from separations of a few micrometers, whereas for graphene at more than an order of magnitude shorter separations. It is worth mentioning also that for two dielectric plates with account of dc conductivity the Lifshitz theory violates^{2,6,56} the third law of thermodynamics (the Nernst heat theorem).

For graphene modeled as two metallic films described by the plasma model under the condition (30), the Casimir free energy is given by Eq. (36). Here the magnitude of the main term is larger by a factor of two than for graphene sheets in Eq. (64). If, however, at least one film is described by the plasma model under the condition (32), we again arrive to the same main term as in Eq. (64) obtained for graphene sheets [see, e.g., Eq. (39)]. Thus, both the Drude and the plasma models can be used to obtain the classical limit for graphene. Furthermore, the Drude-type dielectric permittivity leads to exactly zero contribution of the TE mode at zero frequency, whereas for graphene it is, although small, but not equal to zero. This qualitatively likens graphene to a metallic film described by the plasma model. By and large both the Drude and the plasma dielectric permittivities do not provide a correct quantitative description of such a unique two-dimensional system as graphene.

Now we compare the results of Sec. II for the Casimir interaction between a thin film and a thick plate (semispace) with respective results for a graphene sheet. Using the formalism of a polarization tensor, the Casimir free energy of graphene interacting with a dielectric semispace was calculated in Ref.³⁰. In the classical limit for a gapless graphene it is given

by the asymptotic expression^{23,30}

$$\mathcal{F}(a, T) \approx -\frac{k_B T \text{Li}_3(r_0^{(-2)})}{16\pi a^2} \left[1 - \frac{1}{8\alpha \ln 2} \left(\frac{v_F}{c} \right)^2 \frac{\hbar c}{ak_B T} \right]. \quad (65)$$

This demonstrates another dependence on separation than in the first equation (15) obtained for a dielectric film of thickness d_+ interacting with a dielectric semispace.

The next step is to compare Eq. (65) with the free energy of the classical Casimir interaction between a metallic film and a dielectric semispace. The latter quantity is the same as for metallic and dielectric semispaces. It does not depend on the model of metal used and is given by⁵⁷

$$\mathcal{F}(a, T) \approx -\frac{k_B T \text{Li}_3(r_0^{(-2)})}{16\pi a^2} \quad (66)$$

in accordance with the main contribution to Eq. (65) obtained for a graphene–semispace interaction.

The classical Casimir interaction between a graphene sheet and a metallic semispace is of interest because of possible dependence on the model of metal. If the semispace is described by the Drude model, the free energy of graphene–semispace interaction is given by^{22,23,30}

$$\mathcal{F}(a, T) \approx -\frac{k_B T \zeta(3)}{16\pi a^2} \left[1 - \frac{1}{8\alpha \ln 2} \left(\frac{v_F}{c} \right)^2 \frac{\hbar c}{ak_B T} \right]. \quad (67)$$

If the semispace is described by the plasma model, only a negligible small correction to Eq. (67) is added.³⁰

Let us compare this result with the classical Casimir interaction of the material film with a metallic semispace, both describe by some dielectric permittivities. If the film is made of insulator material, the classical Casimir free energy of its interaction with a metallic plate is given by the first equation (18) and does not depend on the model of metal. As can be seen in Eq. (18), it depends on the film thickness d_+ and differs essentially from the main contribution to Eq. (67). Alternatively, if the film is metallic the classical Casimir free energy depends on the model of a metal. If both the film and the semispace metals are described at low frequencies by the Drude model, the result is^{2,6}

$$\mathcal{F}_D(a, T) \approx -\frac{k_B T \zeta(3)}{16\pi a^2}, \quad (68)$$

i.e., the same as the main contribution in Eq. (67). One should remember, however, that the Lifshitz theory combined with the Drude model violates the Nernst heat theorem.^{43–45}

If both metals are described at low frequencies by the plasma model under the condition (30), one obtains $\mathcal{F}_p \approx 2\mathcal{F}_D$ in disagreement with the main contribution to Eq. (67). When the condition (32) is satisfied, one obtains $\mathcal{F}_p \approx \mathcal{F}_D$ in agreement with Eq. (67) found using the description of graphene by means of the polarization tensor.

VI. CONCLUSIONS AND DISCUSSION

In the foregoing we have considered the classical Casimir interaction between two thin material films made of dielectrics and metals, between a film and a thick plate (semispace), and between two films deposited on substrates. The consideration of a classical limit, where the interaction does not depend on the Planck constant, presents some advantages, because all results can be found in simple analytic form. The problem of the Casimir interaction between thin films has become topical because of increasing interest to the dispersion interactions of graphene. In this area many results were obtained by using the Lifshitz theory and describing graphene sheets in close analogy with material films of nonzero thickness possessing some model dielectric permittivity. Alternatively (and more fundamentally) the reflection coefficients of the electromagnetic oscillations on graphene described by the Dirac model were expressed via the polarization tensor with no recourse to the concept of dielectric permittivity. Some of the results obtained using both these approaches were found to be in mutual disagreement.

In this paper we have shown that the classical limit of the Casimir interaction for two dielectric films with no free charge carriers is different from the classical limit for two dielectric semispaces and depends on film thicknesses. The respective Casimir free energy decreases as an inversely fourth power of separation instead of the inversely second power, as it holds in the classical limit for two dielectric semispaces and for two graphene sheets described by the polarization tensor in the framework of the Dirac model. Thus, modeling of the pristine graphene as an insulating film should be considered as unrealistic.

Another conclusion is that one obtains the correct main contribution to the classical Casimir free energy when the graphene sheets are modeled as material films with metallic-type dielectric permittivity. This, however, is achieved at separations of a few micrometers, i.e., at much larger separations than the classical regime is achieved²² for graphene sheets described by the Dirac model. As a result, at moderate separations between graphene

sheets, which are of most experimental interest, the theoretical predictions using the model of graphene as a dielectric possessing some dc conductivity cannot be considered as enough reliable.

One can also conclude that it is most prospective to investigate the dispersion interactions between graphene sheets, both isolated and deposited on substrates, using the formalism of the polarization tensor. In this connection it is desirable to generalize the quantum electrodynamical formalism to the case when the two-dimensional layer described by the polarization tensor is sandwiched between two material plates described by two different dielectric permittivities.

APPENDIX A

Here we present a few details of analytic derivations related to Sec. IV. We begin from the case of two dielectric films each of which is deposited on a dielectric semispace. From Eqs. (3)–(5) it follows

$$\begin{aligned} R_{\text{TM}}^{(\pm)}(0, k_{\perp}) &= \frac{r_0^{(\pm 1)} + r_0^{(\pm 2, \pm 1)} e^{-2k_{\perp} d_{\pm}}}{1 + r_0^{(\pm 1)} r_0^{(\pm 2, \pm 1)} e^{-2k_{\perp} d_{\pm}}}, \\ R_{\text{TE}}^{(\pm)}(0, k_{\perp}) &= 0, \end{aligned} \quad (\text{A1})$$

where $r_0^{(\pm 1)}$ is defined in Eq. (6) and $r_0^{(-2, -1)}$ is defined in the same way as $r_0^{(2, 1)}$ in Eq. (42). Substituting these definitions in Eq. (A1), using the variable y and expanding in powers of small parameters d_{\pm}/a , one obtains

$$R_{\text{TM}}^{(\pm)}(0, y) \approx r_0^{(\pm 2)} - \frac{\varepsilon_0^{(\pm 2)^2} - \varepsilon_0^{(\pm 1)^2}}{\varepsilon_0^{(\pm 1)} [\varepsilon_0^{(\pm 2)} + 1]^2} \frac{d_{\pm}}{a} y. \quad (\text{A2})$$

From Eq. (A2) it is easily obtainable

$$\begin{aligned} R_{\text{TM}}^{(+)}(0, y) R_{\text{TM}}^{(-)}(0, y) &\approx r_0^{(2)} r_0^{(-2)} \\ &- r_0^{(2)} \frac{\varepsilon_0^{(-2)^2} - \varepsilon_0^{(-1)^2}}{\varepsilon_0^{(-1)} [\varepsilon_0^{(-2)} + 1]^2} \frac{d_-}{a} y - r_0^{(-2)} \frac{\varepsilon_0^{(2)^2} - \varepsilon_0^{(1)^2}}{\varepsilon_0^{(1)} [\varepsilon_0^{(2)} + 1]^2} \frac{d_+}{a} y. \end{aligned} \quad (\text{A3})$$

This is used in the main text to obtain Eq. (55).

Now we present some calculation details for the case of two dielectric films deposited on

metallic semispaces described by the plasma model. From Eqs. (3)–(5) we have

$$R_{\text{TE}}^{(\pm)}(0, y) \approx r_{\text{TE}}^{(\pm 1, \pm 2)}(0, y)e^{-d_{\pm}y/a} \quad (\text{A4})$$

$$\approx (-1 + 2\beta_{\pm 2}y) \left(1 - \frac{d_{\pm}}{a}y\right) \approx -1 + \frac{\delta_{\pm 2}}{a}y + \frac{d_{\pm}}{a}y,$$

where $\delta_{\pm 2} = c/\omega_{p, \pm 2}$, $\omega_{p, \pm 2}$ are the plasma frequencies of the upper and lower metallic semispaces and $\beta_{\pm 2} = \delta_{\pm 2}/(2a)$. From Eq. (A4) one has

$$R_{\text{TE}}^{(+)}(0, y)R_{\text{TE}}^{(-)}(0, y) \approx 1 - \frac{\delta_2 + \delta_{-2} + d_+ + d_-}{a}y, \quad (\text{A5})$$

which, with the help of Eq. (2), leads to

$$\mathcal{F}_{\text{TE}}(a, T) \approx -\frac{k_B T \zeta(3)}{16\pi a^2} \left(1 - 2\frac{\delta_2 + \delta_{-2} + d_+ + d_-}{a}\right). \quad (\text{A6})$$

This is used to obtain Eq. (60) in the main text.

-
- ¹ V. A. Parsegian, *Van der Waals Forces: A Handbook for Biologists, Chemists, Engineers, and Physicists* (Cambridge University Press, Cambridge, 2005).
- ² M. Bordag, G. L. Klimchitskaya, U. Mohideen, and V. M. Mostepanenko, *Advances in the Casimir Effect* (Oxford University Press, Oxford, 2009).
- ³ M. Krech, *The Casimir Effect in Critical Systems* (World Scientific, Singapore, 1994).
- ⁴ V. M. Mostepanenko and N. N. Trunov, *The Casimir Effect and its Applications* (Clarendon, Oxford, 1997).
- ⁵ K. A. Milton, *The Casimir Effect: Physical Manifestations of Zero-Point Energy* (World Scientific, Singapore, 2001).
- ⁶ G. L. Klimchitskaya, U. Mohideen, and V. M. Mostepanenko, *Rev. Mod. Phys.* **81**, 1827 (2009).
- ⁷ A. W. Rodriguez, F. Capasso, and S. G. Johnson, *Nature Photon.* **5**, 211 (2011).
- ⁸ G. L. Klimchitskaya, U. Mohideen, and V. M. Mostepanenko, *Int. J. Mod. Phys. B* **25**, 171 (2011).
- ⁹ E. M. Lifshitz, *Zh. Eksp. Teor. Fiz.* **29**, 94 (1955) [*Sov. Phys. JETP* **2**, 73 (1956)].
- ¹⁰ S. Y. Buhmann, D.-G. Welsch, and T. Kampf, *Phys. Rev. A* **72**, 032112 (2005).
- ¹¹ M. S. Tomaš, *Phys. Lett. A* **342**, 381 (2005).
- ¹² T. Emig, N. Graham, R. L. Jaffe, and M. Kardar, *Phys. Rev. Lett.* **99**, 170403 (2007).

- ¹³ O. Kenneth and I. Klich, *Phys. Rev. B* **78**, 014103 (2008).
- ¹⁴ M. S. Dresselhaus, *Physica Status Solidi (b)* **248**, 1566 (2011).
- ¹⁵ A. H. Castro Neto, F. Guinea, N. M. R. Peres, K. S. Novoselov, and A. K. Geim, *Rev. Mod. Phys.* **81**, 109 (2009).
- ¹⁶ J. F. Dobson, A. White, and A. Rubio, *Phys. Rev. Lett.* **96**, 073201 (2006).
- ¹⁷ I. V. Bondarev and Ph. Lambin, *Phys. Rev. B* **70**, 035407 (2004).
- ¹⁸ E. V. Blagov, G. L. Klimchitskaya, and V. M. Mostepanenko, *Phys. Rev. B* **71**, 235401 (2005).
- ¹⁹ M. Bordag, *J. Phys. A: Math. Gen.* **39**, 6173 (2006).
- ²⁰ M. Bordag, B. Geyer, G. L. Klimchitskaya, and V. M. Mostepanenko, *Phys. Rev. B* **74**, 205431 (2006).
- ²¹ M. Bordag, I. V. Fialkovsky, D. M. Gitman, and D. V. Vassilevich, *Phys. Rev. B* **80**, 245406 (2009).
- ²² G. Gómez-Santos, *Phys. Rev. B* **80**, 245424 (2009).
- ²³ I. V. Fialkovsky, V. N. Marachevsky, and D. V. Vassilevich, *Phys. Rev. B* **84**, 035446 (2011).
- ²⁴ D. Drosdoff and L. M. Woods, *Phys. Rev. B* **82**, 155459 (2010).
- ²⁵ D. Drosdoff and L. M. Woods, *Phys. Rev. A* **84**, 062501 (2011).
- ²⁶ B. E. Sernelius, *Europhys. Lett.* **95**, 57003 (2011).
- ²⁷ J. Sarabadani, A. Naji, R. Asgari, and R. Podgornik, *Phys. Rev. B* **84**, 155407 (2011).
- ²⁸ D. Drosdoff, A. D. Phan, L. M. Woods, I. V. Bondarev, and J. F. Dobson, *Eur. Phys. J. B* **85**, 365 (2012).
- ²⁹ A. D. Phan, L. M. Woods, D. Drosdoff, I. V. Bondarev, and N. A. Viet, *Appl. Phys. Lett.* **101**, 113118 (2012).
- ³⁰ M. Bordag, G. L. Klimchitskaya, and V. M. Mostepanenko, *Phys. Rev. B* **86**, 165429 (2012).
- ³¹ G. L. Klimchitskaya and V. M. Mostepanenko, *Phys. Rev. B* **87**, 075439 (2013).
- ³² G. L. Klimchitskaya, U. Mohideen, and V. M. Mostepanenko, *Phys. Rev. A* **61**, 062107 (2000).
- ³³ L. Duraffourg and P. Andreucci, *Phys. Lett. A* **359**, 406 (2006).
- ³⁴ A. Lambrecht, I. Pirozhenko, L. Duraffourg, and P. Andreucci, *Europhys. Lett.* **77**, 44006 (2007); Err. **81**, 19901 (2008).
- ³⁵ I. Pirozhenko and A. Lambrecht, *Phys. Rev. A* **77**, 013811 (2008).
- ³⁶ M. Boström, C. Persson, and B. E. Sernelius, *Eur. Phys. J. B* **86**, 43 (2013).
- ³⁷ J. Feinberg, A. Mann, and M. Revzen, *Ann. Phys. (N.Y.)* **288**, 103 (2001).

- ³⁸ R. S. Decca, D. López, E. Fischbach, G. L. Klimchitskaya, D. E. Krause, and V. M. Mostepanenko, *Phys. Rev. D* **75**, 077101 (2007).
- ³⁹ R. S. Decca, D. López, E. Fischbach, G. L. Klimchitskaya, D. E. Krause, and V. M. Mostepanenko, *Eur. Phys. J. C* **51**, 963 (2007).
- ⁴⁰ C.-C. Chang, A. A. Banishev, R. Castillo-Garza, G. L. Klimchitskaya, V. M. Mostepanenko, and U. Mohideen, *Phys. Rev. B* **85**, 165443 (2012).
- ⁴¹ A. A. Banishev, G. L. Klimchitskaya, V. M. Mostepanenko, and U. Mohideen, *Phys. Rev. Lett.* **110**, 137401 (2013).
- ⁴² A. A. Banishev, G. L. Klimchitskaya, V. M. Mostepanenko, and U. Mohideen, *Phys. Rev. B* **88**, 155410 (2013).
- ⁴³ V. B. Bezerra, G. L. Klimchitskaya, and V. M. Mostepanenko, *Phys. Rev. A* **65**, 052113 (2002).
- ⁴⁴ V. B. Bezerra, G. L. Klimchitskaya, and V. M. Mostepanenko, *Phys. Rev. A* **66**, 062112 (2002).
- ⁴⁵ V. B. Bezerra, G. L. Klimchitskaya, V. M. Mostepanenko, and C. Romero, *Phys. Rev. A* **69**, 022119 (2004).
- ⁴⁶ A. O. Sushkov, W. J. Kim, D. A. R. Dalvit, and S. K. Lamoreaux, *Nature Phys.* **7**, 230 (2011).
- ⁴⁷ D. Garcia-Sanchez, K. Y. Fong, H. Bhaskaran, S. Lamoreaux, and H. X. Tang, *Phys. Rev. Lett.* **109**, 027202 (2012).
- ⁴⁸ V. B. Bezerra, G. L. Klimchitskaya, U. Mohideen, V. M. Mostepanenko, and C. Romero, *Phys. Rev. B* **83**, 075417 (2011).
- ⁴⁹ G. L. Klimchitskaya and V. M. Mostepanenko, *Int. J. Mod. Phys. A* **26**, 3944 (2011).
- ⁵⁰ G. L. Klimchitskaya, M. Bordag, E. Fischbach, D. E. Krause, and V. M. Mostepanenko, *Int. J. Mod. Phys. A* **26**, 3918 (2011).
- ⁵¹ G. L. Klimchitskaya, M. Bordag, and V. M. Mostepanenko, *Int. J. Mod. Phys. A* **27**, 1260012 (2012).
- ⁵² M. Bordag, G. L. Klimchitskaya, and V. M. Mostepanenko, *Phys. Rev. Lett.* **109**, 199701 (2012).
- ⁵³ M. Chaichian, G. L. Klimchitskaya, V. M. Mostepanenko, and A. Tureanu, *Phys. Rev. A* **86**, 012515 (2012).
- ⁵⁴ B. E. Sernelius, *Phys. Rev. B* **85**, 195427 (2012).
- ⁵⁵ J. Sarabadani, A. Naji, R. Asgari, and R. Podgornik, *Phys. Rev. B* **86**, 239905(E) (2013).
- ⁵⁶ B. Geyer, G. L. Klimchitskaya, and V. M. Mostepanenko, *Phys. Rev. D* **72**, 085009 (2005).
- ⁵⁷ B. Geyer, G. L. Klimchitskaya, and V. M. Mostepanenko, *Ann. Phys. (N.Y.)* **323**, 291 (2008).

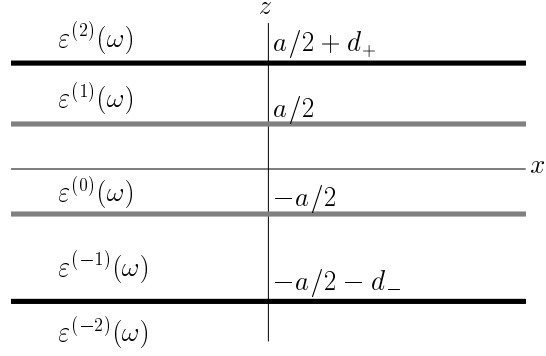


FIG. 1: Stratified medium consisting of three layers of finite thickness d_- , a , and d_+ with dielectric permittivities $\varepsilon^{(-1)}(\omega)$, $\varepsilon^{(0)}(\omega)$, and $\varepsilon^{(1)}(\omega)$, enclosed between two semispaces $z \leq -a/2 - d_-$ and $z \geq a/2 + d_+$ with dielectric permittivities $\varepsilon^{(-2)}(\omega)$ and $\varepsilon^{(2)}(\omega)$, respectively.